PROCEEDINGS OF SCIENCE

Searches for diboson resonances with ATLAS (VV, VH and HH, excl. diphoton resonance)

Kristian Anders Gregersen*
University College London (UK)
E-mail: kristian.anders.gregersen@cern.ch

This document summarises ATLAS searches for resonances decaying to diboson final states, VV, VH and HH, where V is either a W or a Z boson and H is the Standard Model Higgs boson. The results obtained are based on the full 2015 dataset corresponding to an integrated luminosity of 3.2 fb^{-1}. No discrepancies with respect to the Standard Model expectations are observed and thus 95% confidence level exclusion limits are set on the production cross section times branching ratios in a number of benchmark scenarios, including Heavy Vector Triplet, Randall-Sundrum Graviton and Extended Higgs sector models.

Fourth Annual Large Hadron Collider Physics
13-18 June 2016
Lund, Sweden

PoS(LHCP2016)094

*Speaker.

1. Introduction

Many scenarios of physics beyond the Standard Model (SM) predict the existence of heavy particles that preferentially couple to the Higgs boson and massive gauge bosons, the production of which would produce striking signatures at the Large Hadron Collider (LHC). In this document, the results from recently performed searches for resonant production of VV, VH and HH are summarised. They are carried out using data taken with the ATLAS detector [1] during the 2015 run of the LHC, corresponding to an integrated luminosity of 3.2 fb^{-1}.

In order to asses the sensitivity of the searches, to optimise the event selections, and for comparison with the data, a number of models are used as benchmarks. An extended Higgs sector serves as benchmark model for spin-0 resonances, Heavy Vector Triplets (HVT) Model A (which has comparable branching fractions to fermions and gauge bosons) and Model B (which has enhanced couplings to gauge bosons) for spin-1 in form of W' and Z' [2], and bulk Randall-Sundrum Gravitons (RSG) [3] for spin-2 resonances.

The sensitivity of searches for new heavy resonances critically depends on the efficient reconstruction and identification of their unique detector signatures. If these new states are sufficiently heavy their decay products will be highly boosted in the rest frame of the detector. The defining property of the decay of a boosted object is that the decay products appear collimated in the momentum direction of the boosted mother particle. For a two-body decay of a SM particle the geometrical distance between the child particles can be approximated by $\Delta R = \sqrt{\Delta\eta^2 + \Delta\phi^2} \approx 2m/p_T$, where m and p_T are the mass and transverse momentum of the parent particle, respectively. For a high p_T hadronically decaying V or Higgs boson this means that it is difficult to resolve the decay products from the energy deposits in the calorimeters with the standard ATLAS anti-k_t algorithm [4] with $R = 0.4$. In order to resolve this the boson is instead reconstructed as a single jet using the anti-k_t algorithm with $R = 1$. These jets are referred to as large-R jets. A *trimming* algorithm [5] is applied to the large-R jets in order to remove noise from soft radiation, retaining only components carrying at least 5% of the original jet's energy.

In signal events the substructure in large-R jets follows a distinct two-prong pattern. For hadronically decaying W and Z bosons this information is exploited together with the trimmed jet mass in a vector boson tagging algorithm [6] which provides a single discriminant variable to cut on. Higgs bosons decaying to bottom quarks are identified by applying a dedicated Higgs-tagging algorithm [7] to the large-R jets. This algorithm proceeds by ghost-associating [8] anti-k_t jets ($R = 0.2$) reconstructed from tracks in the Inner Detector (ID) and applying a b-tagging algorithm [9] re-optimised for Run 2 to these track-based jets in order to identify the b hadrons from the Higgs boson decay. The operating point of the b-tagging algorithm is chosen such that the b-tagging efficiency for jets containing b-hadrons is 77%. In addition, a mass window cut around the SM Higgs mass of 125 GeV is applied to the large-R jet.

The next sections summarise the individual searches presented in this talk. Section 2 gives the results for the VV searches [10], followed by the results for VH [11] in section 3. Section 4 presents the results for HH [12], and finally a short summary is given in section 5.

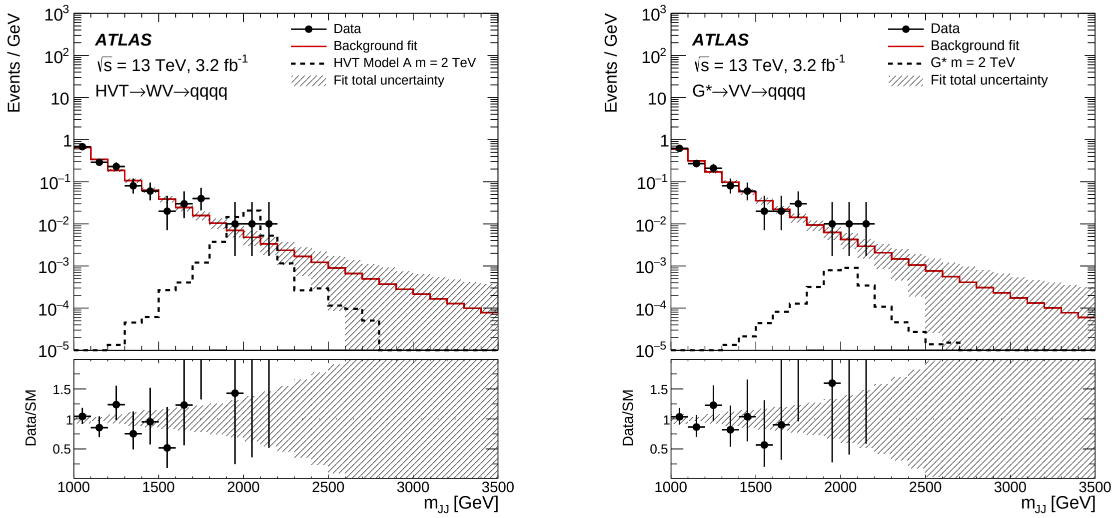

(a) (b)

Figure 1: Distribution of events passing the event selection as function of the invariant mass of the VV system for (a) the HVT and (b) the RSG signal regions in the fully hadronic VV analysis. Both figures are taken from Ref. [10].

2. VV resonances

The searches for heavy resonances decaying to VV are carried out in four distinct channels based on the decays of the vector bosons: $VV \to qqqq$, $VV \to llqq$, $VV \to l\nu qq$ or $VV \to \nu\nu qq$, where the first decay channel is referred to as the fully hadronic channel and the other channels collectively are referred to as the semi-leptonic decay channels where l denotes a muon or electron. Section 2.1 presents the event selection for the fully hadronic channel, section 2.2 presents the selections in the semi-leptonic channels, and finally the results for the combination of the individual searches are given is section 2.3.

2.1 Fully hadronic VV

The event selection in the fully hadronic decay channel requires two large-R jets with $p_T > 450$ (200) GeV for the leading (sub-leading) jet. The vector boson tagger mentioned in the introduction is applied at a 50% efficiency working point giving a QCD rejection factor between 40–70 per jet depending on the p_T of the jet. Further requirements are applied on the number of tracks in the two jets, their rapidity difference and their p_T asymmetry. Three overlapping signal regions are defined for WW, WZ and ZZ based on the jet masses.

The SM background, consisting mostly of QCD, is described using a power-law function, the shape of which is validated in control regions. Figures 1a and 1b show the distribution of the data compared to the background estimate for the invariant mass of the VV system for the HVT and RSG searches, respectively.

2.2 Semi-leptonic VV

The hadronically decaying V boson is reconstructed in a large-R jet with $p_T > 200$ GeV and the

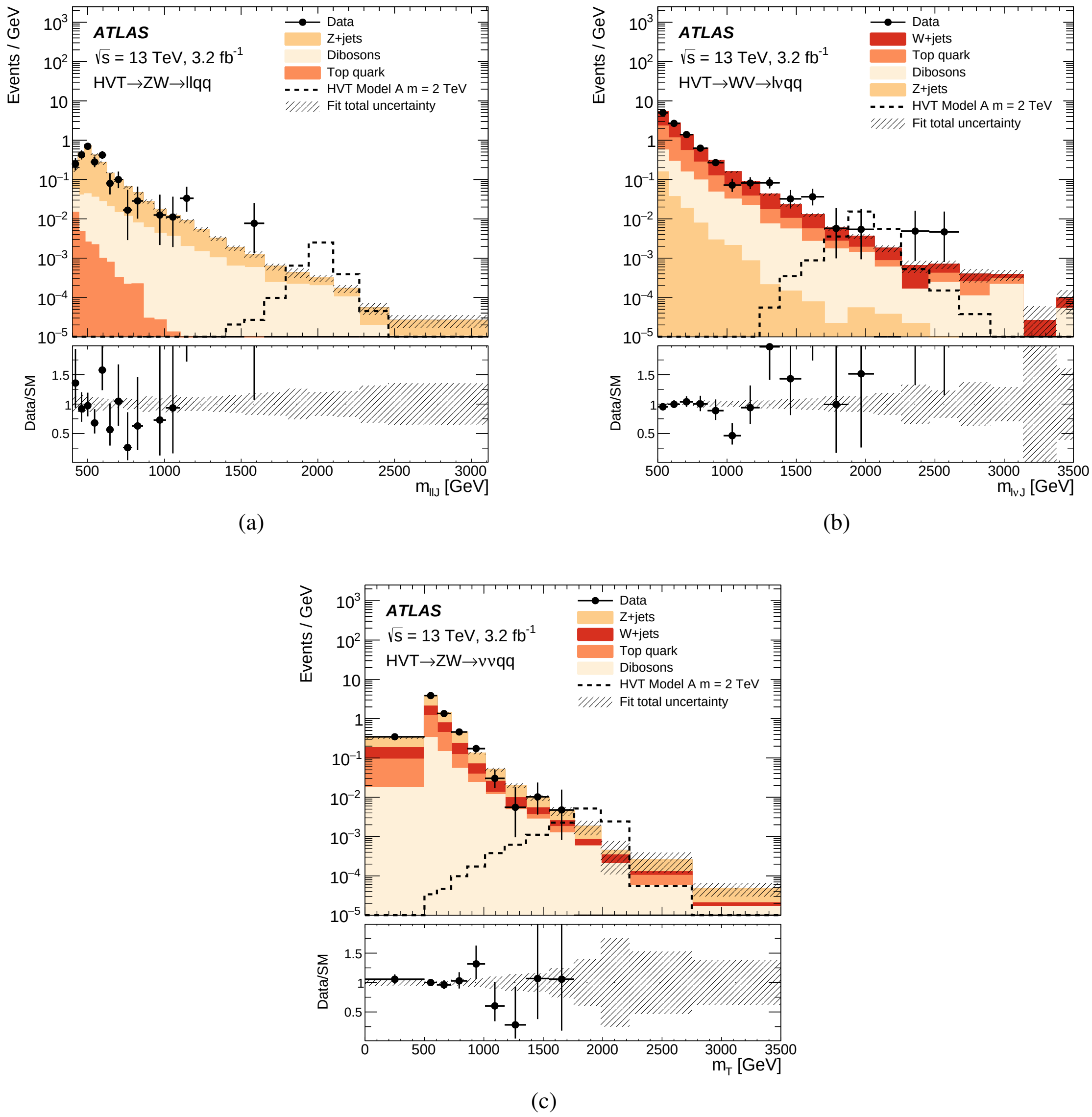

Figure 2: Distribution of events passing the event selection as function of the invariant and the transverse masses of the VV system for the HVT signal regions for (a) $VV \to llqq$, (b) $VV \to l\nu qq$ and (c) $VV \to \nu\nu qq$. All figures are taken from Ref. [10].

same boson-tagging requirements are imposed as in the fully hadronic decay channel. In the $Z \to \nu\nu$ channel, a veto is applied on the presence of muons and electrons with transverse momentum, p_T, larger than 7 GeV and the event is required to have missing transverse energy, E_T^{miss}, greater than 200 GeV. Additional angular cuts on the jets and E_T^{miss} are imposed to reject the multijet background from QCD. In the $W \to l\nu$ channel exactly one muon or electron is required with $p_T > 25$ GeV and tight identification and isolation criteria. In the $Z \to ll$ channel exactly two muons or two electrons are required with $p_T > 25$ GeV and looser identification criteria compared to the $W \to l\nu$ channel. In the $Z \to ll$ and $W \to l\nu$ channels it is required that the p_T of both V bosons is larger than 0.4 times the invariant mass of the VV system. In the $Z \to \nu\nu$ and $W \to l\nu$

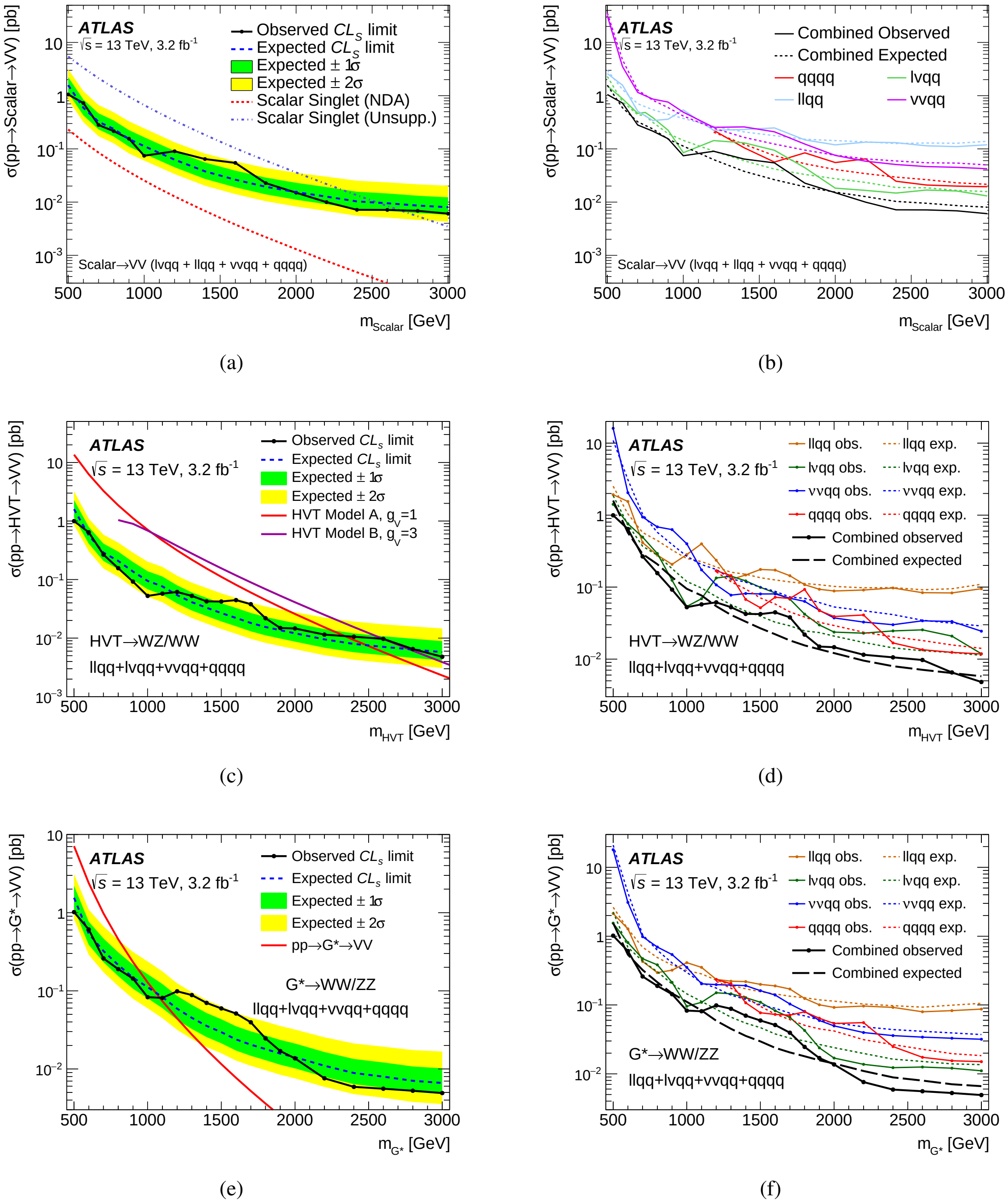

Figure 3: Observed and expected 95% CL limits on the cross section times branching ratio to diboson final states for (a) a narrow-width scalar resonance, (c) a HVT scenario, and (d) bulk RSG, with the corresponding decompositions into the contributions from the different channels in (b), (d) and (f), respectively. All figures are taken from Ref. [10].

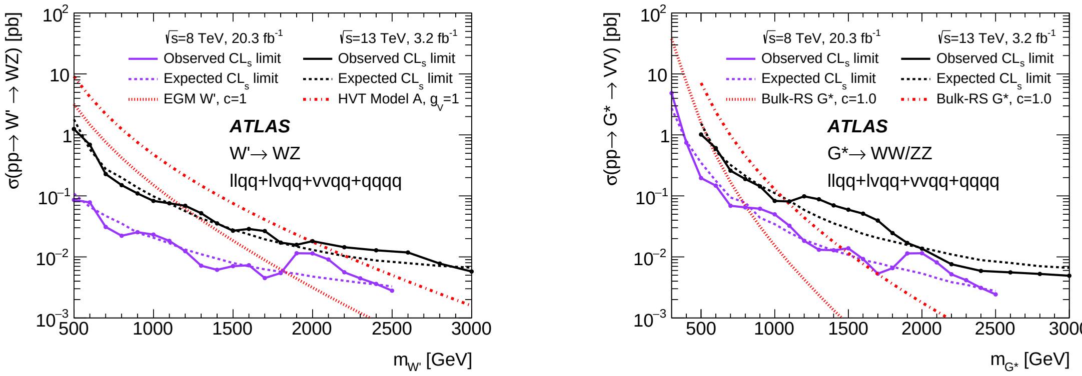

(a) (b)

Figure 4: Comparison of 8 TeV and 13 TeV exclusion limits for (a) a $G*$ decaying to WW/ZZ in the bulk RSG model and (b) a W' decaying to WZ in the HVT Model A. Both figures are taken from Ref. [10].

channels a veto on b-jets is applied to reject the $t\bar{t}$ background.

The SM backgrounds are simulated using Monte Carlo (MC) generators and are validated in control regions. Figure 2 show the distribution of the data compared to the background estimate for the invariant and transverse masses of the VV system for the three decay channels in the signal regions.

2.3 Combined Results

No significant excess over the background is observed in the signal regions and thus 95% confidence level (CL) exclusion limits on the production cross section times the branching ratio are set, as shown in figure 3. Figure 4 shows a comparison of the limits obtained in previous analyses (purple) at 8 TeV against the limits obtained in the present analyses at 13 TeV (black).

3. VH resonances

The search for VH resonances is considered for the leptonic decays of the V boson and the Higgs decay to b-quarks, giving three final states: $VH \to llb\bar{b}$, $l\nu b\bar{b}$ and $\nu\nu b\bar{b}$. The V boson is reconstructed using similar requirements as in the semileptonic VV searches and the Higgs boson is reconstructed using the Higgs-tagging requirements outlined in the introduction. The p_T of the large-R jet is reqired to be larger than 250 GeV and $|\eta| < 2$. The signal region is defined by applying a cut on the jet mass of $75 < m_J < 145$ GeV. The mass side-bands and additional b-tags in the event are used to define control regions. The signal region is divided into one- and two-b-tag regions in order to include signal events where one of the b-hadrons is not tagged.

The SM backgrounds are simulated with MC and are validated in control regions. Figure 2 show the distribution of the data compared to the background estimate for the invariant and the transverse masses of the VH system for the three decay channels in the signal regions.

PoS(LHCP2016)094

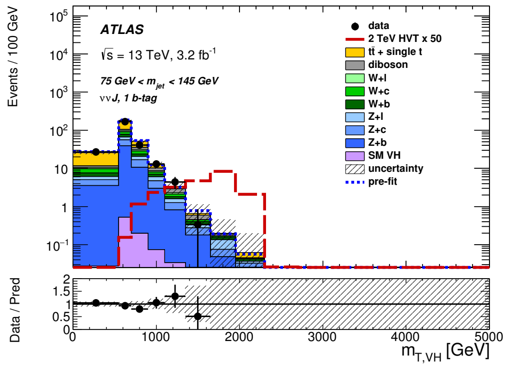

(a)

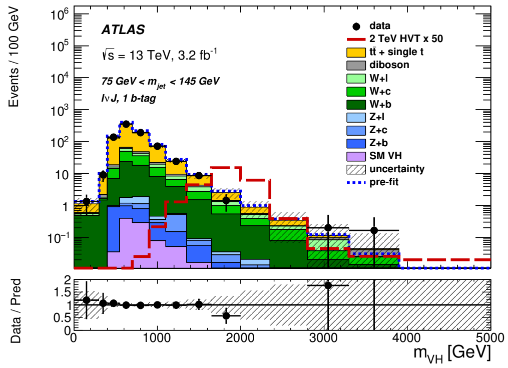

(b)

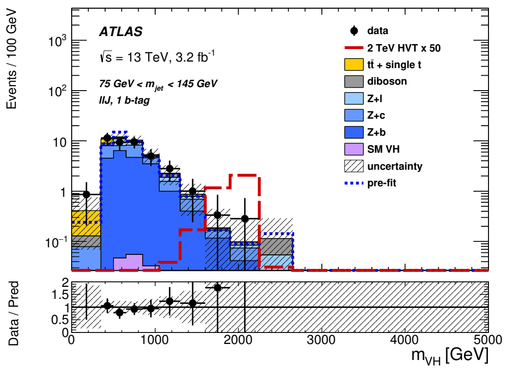

(c)

Figure 5: Distribution of reconstructed VH transverse mass and invariant mass, for (a) $VH \to \nu\nu b\bar{b}$, (b) $VH \to l\nu b\bar{b}$, and (c) $VH \to llb\bar{b}$. All figures are taken from Ref. [11].

No significant excess over the SM background is observed, and thus 95% CL exclusion limits are set on the production cross section times branching fraction in the HVT model as shown in figure 6.

4. *HH* resonances

The search for HH resonances is done in both the boosted and resolved regimes, covering the high and low energy regimes, respectively. In the boosted analysis events are required to have two large-R jets with $p_T > 350(250)$ GeV for the leading (sub-leading) jet, $|\eta| < 2$ and an invariant mass larger than 50 GeV. The resolved analysis requires four b-tagged jets reconstructed with the anti-k_t algorithm with $R = 0.4$ using a b-tagging operating point corresponding to a 70% b-tagging efficiency on jets containing b-hadrons. The jets are required to have $p_T > 40$ GeV and $|\eta| < 2.5$, and are combined in pairs requiring that $\Delta R < 1.5$. The two leading dijets from this pairing form the Higgs candidates and are further required to pass a p_T cut which depends on the invariant mass of the HH system, the cut value being larger for larger HH masses.

For both the boosted and the resolved analyses the dominant background is QCD multijet which is estimated in a side band region and validated in a validation region in the m_{H_1}, m_{H_2} plane,

PoS(LHCP2016)094

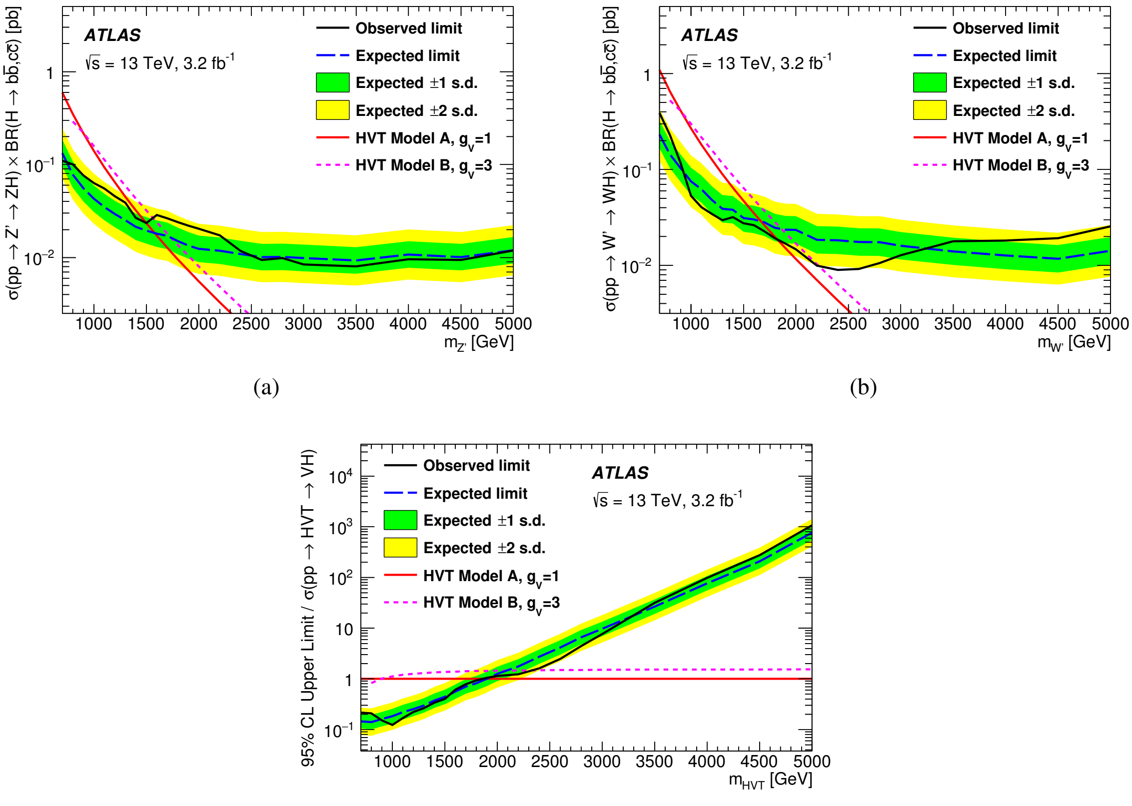

(a) (b) (c)

Figure 6: Upper limits at 95% CL on the production cross section of (a) Z' times its branching fraction to ZH and (b) W' times its branching fraction to WH, and both times the branching ratio $BR(H \to b\bar{b}/c\bar{c})$. Figure (c) shows the upper limits for the scaling factor of the production cross section for V' times its branching fraction to WH/ZH in HVT model A. All figures are taken from Ref. [11].

where m_H refers to the invariant mass of the Higgs candidate. As seen in figures 7a and 7b, no significant excess is observed in the signal regions and thus 95% CL exclusion limits are set on the production cross section times branching ratio in the RSG model as shown in figure 7c. An interesting feature in this limit plot is seen at very high graviton mass where the limits degrades due to two effects: the ghost-associated track-jets used in the Higgs-tagging algorithm described in the introduction start to merge; the b-tagging efficiency drops at very high jet p_T due to resolution effects as the tracks become extremely collimated.

5. Summary

Searches for resonances decaying to diboson final states, VV, VH and HH using ATLAS data from the 2015 run at the LHC have been presented. No discrepancies with respect to the Standard Model expectations are observed and thus 95% CL exclusion limits are set on the production cross section times branching ratios in a number of benchmark scenarios. For VV searches, the data exclude a scalar singlet with mass below 2650 GeV, a HVT with mass below 2600 GeV, and a bulk

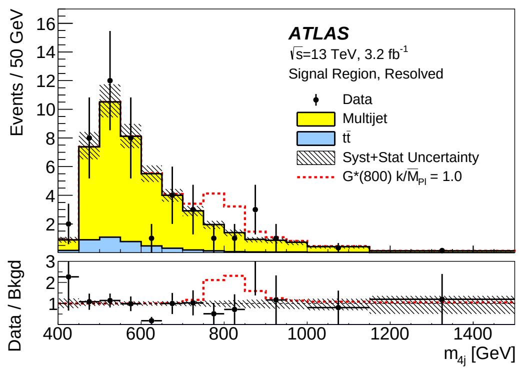

(a)

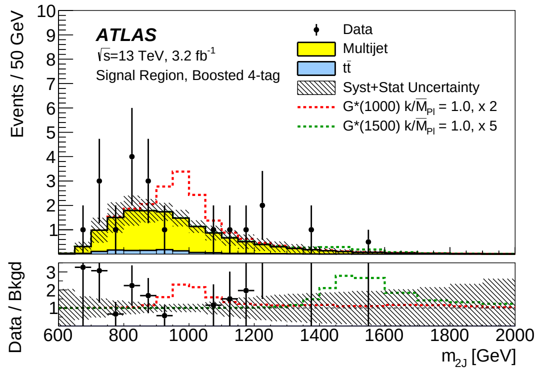

(b)

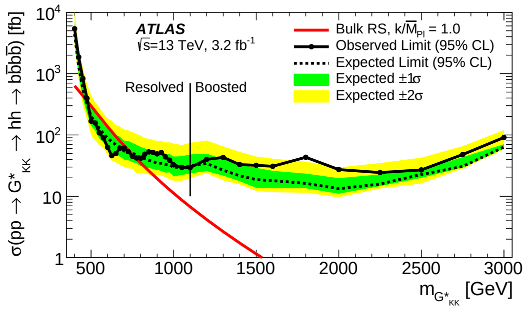

(c)

Figure 7: Dijet mass distributions in the signal regions for (a) the resolved analysis and (b) the 4-tag boosted analysis. The expected and observed upper limit at 95% CL for $pp \to G^*_{\mathrm{KK}} \to HH \to b\bar{b}b\bar{b}$ in the RSG model with $k/M_{Pl} = 1$. The limits from the two individual analyses, the boosted and the resolved, are stitched together at the mass points where they give the same result, as indicated in the plot by the vertical line at M 1100 GeV. All figures are taken from Ref. [12].

RGS mass below 1100 GeV for $k/M_{Pl} = 1$. For VH searches, the data excludes Z' masses below 1490 (1580) GeV and W' masses below 1750 (2220) GeV for HVT Model A (B). For HH searches, the data excludes a bulk RSG mass above 600 Gev and below 770 GeV for $k/M_{Pl} = 1$.

References

[1] ATLAS Collaboration, *The ATLAS Experiments at the CERN Large Hadron Collider* JINST 3 (2008) S08003.

[2] D. Pappadopulo, A. Thamm, R. Torre, A. Wulzer, *Heavy vector triplets: bridging theory and data*, JHEP 9 (2014) 60, arXiv:1402.4431 [hep-ph].

[3] K. Agashe, H. Davoudiasl, G. Perez, A. Soni, *Warped gravitons at the CERN LHC and beyond*, Phys. rev. D76 (2007) 036006, arXiv:hep-ph/0701186.

[4] M. Cacciari, G. P. Salam, G. Soyez, *The anti-k_t jet clustering algorithm*, JHEP 4 (2008) 063, arXiv:0802.1189 [hep-ph].

[5] D. Krohn, J. Thalr, L.-T. Wang, *Jet trimming*, JHEP 2 (2010) 84, arXiv:0912.1342 [hep-ph].

[6] ATLAS Collaboration, *Identification of Boosted, Hadronically-Decaying W and Z Bosons in $\sqrt{s} = 13$ TeV Monte Carlo Simulations for ATLAS*, ATL-PHYS-PUB-2015-033, *https://cds.cern.ch/record/2041461*

[7] ATLAS Collaboration, *Expected Performance of Boosted Higgs ($\rightarrow b\bar{b}$) Boson Identification with the ATLAS Detector at $\sqrt{s} = 13$ TeV*, ATL-PHYS-PUB-2015-035, *https://cds.cern.ch/record/2042155*

[8] M. Cacciari, G. P. Salam, G. Soyez, *The Catchment Area of Jets*, JHEP 0804 (2008) 005, arXiv:0802.1188

[9] ATLAS Collaboration, *Expected performance of the ATLAS b-tagging algorithms in Run-2*, ATL-PHYS-PUB-2015-022, *https://cds.cern.ch/record/2037697*

[10] ATLAS Collaboration, *Searches for heavy diboson resonance in pp collisions at $\sqrt{s} = 13$ TeV with the ATLAS detector*, arXiv:1606.04833 [hep-ex]

[11] ATLAS Collaboration, *Search for new resonances decayig to a W or Z boson and a Higgs boson in the $l^+l^-b\bar{b}$, $l\nu b\bar{b}$, and $\nu\nu b\bar{b}$ channels with pp collisions at $\sqrt{s} = 13$ TeV with the ATLAS detector*, arXiv:1607.05621 [hep-ex]

[12] ATLAS Collaboration, *Search for pair production of Higgs bosons in the bbbb final state using proton - proton collisions at $\sqrt{s} = 13$ TeV with the ATLAS detector*, arXiv:1606.04782 [hep-ex]